Original Article | Cardiovascular Imaging

eISSN 2005-8330
https://doi.org/10.3348/kjr.2023.0061
Korean J Radiol 2023;24(9):827-837

Korean Journal of Radiology
KJR

Non-Contrast Cine Cardiac Magnetic Resonance Derived-Radiomics for the Prediction of Left Ventricular Adverse Remodeling in Patients With ST-Segment Elevation Myocardial Infarction

Xin A[1,2], Mingliang Liu[3], Tong Chen[1,2], Feng Chen[4], Geng Qian[1,2], Ying Zhang[2], Yundai Chen[2]

[1]Chinese People's Liberation Army General Hospital, Chinese People's Liberation Army Medical School, Beijing, China
[2]The Senior Department of Cardiology, the Sixth Medical Center, Chinese People's Liberation Army General Hospital, Beijing, China
[3]Nankai University, School of Medicine, Tianjin, Nankai, China
[4]Department of Computer Science, the University of Adelaide, Adelaide, Australia

Objective: To investigate the predictive value of radiomics features based on cardiac magnetic resonance (CMR) cine images for left ventricular adverse remodeling (LVAR) after acute ST-segment elevation myocardial infarction (STEMI).

Materials and Methods: We conducted a retrospective, single-center, cohort study involving 244 patients (random-split into 170 and 74 for training and testing, respectively) having an acute STEMI (88.5% males, 57.0 ± 10.3 years of age) who underwent CMR examination at one week and six months after percutaneous coronary intervention. LVAR was defined as a 20% increase in left ventricular end-diastolic volume 6 months after acute STEMI. Radiomics features were extracted from the one-week CMR cine images using the least absolute shrinkage and selection operator regression (LASSO) analysis. The predictive performance of the selected features was evaluated using receiver operating characteristic curve analysis and the area under the curve (AUC).

Results: Nine radiomics features with non-zero coefficients were included in the LASSO regression of the radiomics score (RAD score). Infarct size (odds ratio [OR]: 1.04 (1.00–1.07); $P = 0.031$) and RAD score (OR: 3.43 (2.34–5.28); $P < 0.001$) were independent predictors of LVAR. The RAD score predicted LVAR, with an AUC (95% confidence interval [CI]) of 0.82 (0.75–0.89) in the training set and 0.75 (0.62–0.89) in the testing set. Combining the RAD score with infarct size yielded favorable performance in predicting LVAR, with an AUC of 0.84 (0.72–0.95). Moreover, the addition of the RAD score to the left ventricular ejection fraction (LVEF) significantly increased the AUC from 0.68 (0.52–0.84) to 0.82 (0.70–0.93) ($P = 0.018$), which was also comparable to the prediction provided by the combined microvascular obstruction, infarct size, and LVEF with an AUC of 0.79 (0.65–0.94) ($P = 0.727$).

Conclusion: Radiomics analysis using non-contrast cine CMR can predict LVAR after STEMI independently and incrementally to LVEF and may provide an alternative to traditional CMR parameters.

Keywords: Radiomics analysis; ST-elevated myocardial infarction; Percutaneous coronary intervention; Cardiac magnetic resonance imaging; Left ventricular adverse remodeling

INTRODUCTION

Left ventricular (LV) dysfunction and long-term remodeling in patients with ST-segment elevation myocardial infarction (STEMI) are essential intermediate pathophysiological changes in the development of heart

Received: January 17, 2023 **Revised:** May 26, 2023 **Accepted:** June 15, 2023
Corresponding author: Yundai Chen, MD, PhD, The Senior Department of Cardiology, the Sixth Medical Center, Chinese People's Liberation Army General Hospital, No. 6 Fucheng Road, Beijing 100853, China
• E-mail: cyundai@vip.163.com

failure, which are associated with the severity of myocardial injury [1-3]. Early identification of LV adverse remodeling (LVAR) and its prognostic determinants could improve the accuracy of postoperative monitoring and inform individualized management for high-risk patients [4,5]. Cardiac magnetic resonance (CMR) is the gold standard for in vivo assessment of myocardial injury, with CMR markers of myocardial injury, including infarct size [6], microvascular obstruction (MVO) [1], and intramyocardial hemorrhage [7], being predictive of LVAR after myocardial infarction (MI). However, contrast media use in late gadolinium enhancement (LGE) CMR imaging is contraindicated in patients with severe renal damage. Therefore, quantitative CMR measures, particularly those based on contrast-free methods, are increasingly used [8,9]. To date, much of the quantitative information extracted from CMR images has not been fully explored. Considering the substantial overlap between healthy and various disease conditions, a strategy to optimize the use of the data available in CMR images is necessary.

Radiomics analysis is the mathematical quantification of pixel distribution within an image to provide new insights into the association between individual data heterogeneity, clinical outcomes, and treatment response [10,11]. CMR-based radiomics analysis is increasingly used for in vivo myocardial tissue evaluation in various cardiac pathologies [12]. Within the context of STEMI, cine-based radiomics analysis allows the detection of the presence and transmurality of myocardial scars [13,14] and the differentiation of tissue abnormalities that occur during the acute and chronic phases post-infarction [15,16]. However, the predictive efficacy of cine-based radiomics analysis for LVAR, especially in comparison with traditional CMR parameters, remains to be clarified. Accordingly, this study aimed to identify the radiomics features of cine CMR images predictive of LVAR post-revascularization after acute STEMI and to use this information to establish a model to predict LVAR.

MATERIALS AND METHODS

Ethics Statement

This retrospective study was approved by the Ethics Committee of the Chinese People's Liberation Army General Hospital (IRB number: S2021-126-02). The requirement for informed consent was waived.

Study Sample

A retrospective study was conducted among 244 patients aged 18 to 80 years with a diagnosis of STEMI [17] and who underwent CMR examination at 7 ± 2 days and 6 months after percutaneous coronary intervention (PCI) at Chinese People's Liberation Army General Hospital between January 2014 and December 2019. The exclusion criteria included contraindications for CMR (such as claustrophobia, implanted cardiac defibrillator, and gadolinium allergy), history of revascularization therapy (including PCI and coronary artery bypass grafting) within the past 6 months, bundle branch or fascicular block, severe heart valve disease, known cardiomyopathy, and insufficient electrocardiogram data. Figure 1 depicts the study workflow. According to whether adverse LV remodeling occurred, the study sample of 244 participants was randomly divided into training and testing groups, using a 7:3 ratio, with 170 patients (adverse remodeling vs. no adverse remodeling: 37 vs. 133) in the training set and 74 (adverse remodeling vs. no adverse remodeling: 17 vs. 57) in the testing set.

CMR Acquisition and Quantification of LV End-Diastolic Volume

CMR examinations were performed within 7 ± 2 days and 6 months post-PCI after acute STEMI using a 1.5T scanner (Achieva, Philips Medical Systems). A detailed description of the CMR protocol is provided in the supplementary methods (Supplementary Material). Imaging analysis was performed according to current guidelines [18]. Cine CMR imaging was performed with steady-state free precession continuously covering the short axis from the mitral annulus to the apical level in the two- and 4- chamber views using the following parameters: repetition time = 3.73 ms, echo time = 1.87 ms, flip angle = 60°, slice thickness 8.0 mm. The cardiac phases of end-systole and end-diastole were determined by automatically identifying the smallest and largest cavity sizes of the LV in consecutive short axis slices and two-, three-, and 4-chamber orientation cine images. The LV mass assessment did not include the papillary muscles or slow-flowing blood in the trabeculae. All the outlined myocardial borders were manually adjusted by a radiologist. The change in LV end-diastolic volume (EDV) during the follow-up period was calculated as the difference between the LV-EDV at the follow-up time points from the baseline value and normalized to the baseline value (delta LV-EDV [%]/baseline LV-EDV), with a value ≥ 20% indicative of LVAR [19]. LVEF was calculated by dividing the stroke volume by the LV-EDV.

https://doi.org/10.3348/kjr.2023.0061

Korean Journal of Radiology
KJR

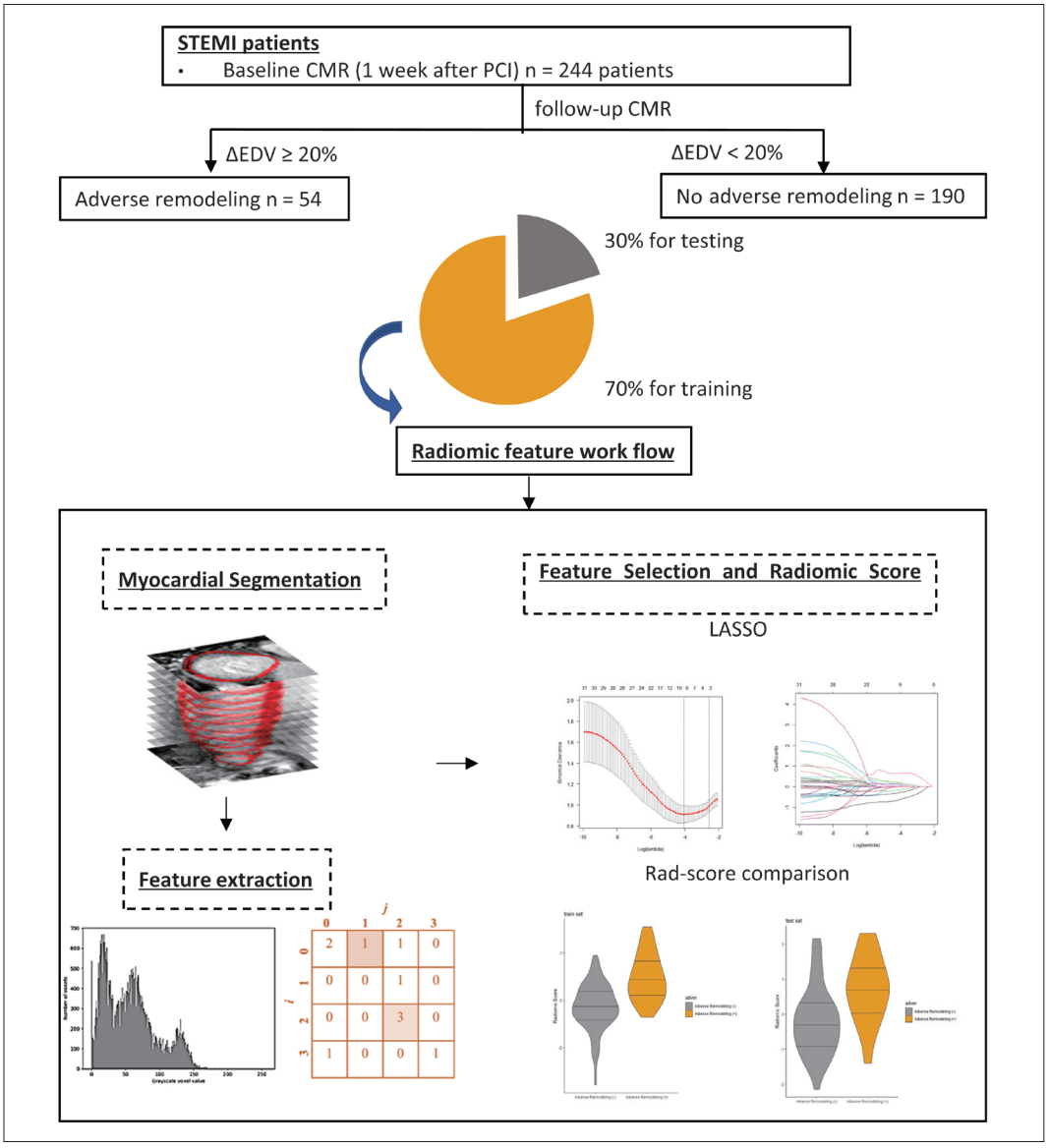

Fig. 1. The study workflow. According to whether adverse LV remodeling occurred, the study sample of 244 participants was randomly divided into training and testing groups, using a 7:3 ratio. Radiomics features were extracted from the one week CMR cine images after LV myocardial segmentation. LASSO regression was used to select most predictive features for adverse LV remodeling. We then compared Radiomic score in patients with and without adverse LV remodeling. LV = left ventricular, STEMI = ST-segment elevation myocardial infarction, CMR = cardiac magnetic resonance, PCI = percutaneous coronary intervention, EDV = end-diastolic volume, LASSO = least absolute shrinkage and selection operator regression

CMR Segmentation and Radiomics Analysis

All radiomic analyses were based on CMR examination within 7 ± 2 days post-PCI after SETMI. LV endocardial and epicardial contours were automatically delineated in the end-diastolic phase using CVI42 (version 5.12.1; Circle Cardiovascular Imaging Inc.). The LV contour was then manually corrected as needed, applying the following principles: slices inclusion with more than 50% circumferential LV while excluding papillary muscles and slow-flowing blood among the trabeculae. The LV myocardium in the end-diastolic phase was defined as the regions of interest (ROIs) using ITK-SNAP (www.itksnap.org) for radiomic analysis. In order to evaluate the radiomics feature reproducibility, the ROI delineation was repeated twice in 45 patients (selected at random) by the same reader for intra-observer reliability and a second reader for inter-observer reliability. The ROIs were delineated by readers who were blinded to the patient's clinical information and endpoints.

Pyradiomics (https://pyradiomics.readthedocs.io/en/

 https://doi.org/10.3348/kjr.2023.0061

latest/) was used to preprocess images and extract the radiomic features using the program's default settings [20]. Before extracting the radiomics features, three preprocessing steps were performed on the original images. 1) The noise effect on the normalized image contrast was eliminated by clipping grayscale values greater than the 99.5th percentile and less than the 0.05th percentile. 2) All images were resampled using B-sample interpolation, and the intensities were further normalized using a box width fixed at 25. 3) The images are normalized using the Z-score (mean/variance of image intensities) so that the imported image intensities are normally distributed.

With that, 1550 radiomics features were retrieved. In order to reduce the influence of range, z-scores were used to standardize all the radiomic features, and features with an intra-class correlation (ICC) coefficient > 0.7 were retained, while features with high collinearity were excluded, leaving 340 features for subsequent analysis.

The least absolute shrinkage and selection operator (LASSO) regression was then used for feature selection and to develop the radiomics score (RAD score). The RAD score was constructed by linearly integrating the final specified radiomics features with their associated coefficients [21].

Statistical Analysis

After the Shapiro-Wilk test, normally distributed continuous variables were presented as mean ± standard deviation, with between-group differences evaluated using the unpaired Student's *t*-test. Non-normally distributed variables are presented as median (Q1–Q3), with between-group differences evaluated using the Kruskal–Wallis test. Chi-square or Fisher's exact test was used to assess between-group differences in categorical variables, expressed as frequencies (proportions). Univariable and multivariable logistic regression analyses were used to assess predictors of LVAR. Variables with a *P*-value < 0.05 in the univariable logistic regression were subsequently included in the multivariable models using the stepwise forward method. In order to explore the additional value of RAD score in comparison to the LVEF and LGE-CMR parameters, combined logistic regression models were developed. Model 1 included RAD score and LVEF, whereas Model 2 incorporated MVO, infarct size, and LVEF. Furthermore, the models were validated using a five-fold cross-validation. Receiver operating characteristic (ROC) curves were used to evaluate the ability of the variables to distinguish between patients with and without LVAR, with the best cutoff for each variable determined by the highest Youden index value. Decision curve analysis was used to evaluate the clinical usefulness of the models. All statistical analyses were performed using R software (version 4.0.2, R Project for Statistical Computing, https://www.r-project.org) and Python (version 3.6, The Python Software Foundation).

RESULTS

Baseline Characteristics and CMR Findings

The baseline characteristics of 244 patients (age: 57.0 ± 10.3 years; 88.5% males) are presented in Table 1. The demographics, clinical status at recruitment, and CMR parameters did not differ significantly between the training and testing groups. The baseline characteristics of the patients stratified by LVAR status in the training and testing sets are presented in Supplementary Table 1.

Radiomics Signatures and the Construction of the RAD Score

A total of 340 radiomics features were included in the analysis after ICC evaluation and collinearity testing. The names of the feature families (categories) and the number of extracted texture features for each family are provided in Supplementary Tables 2 and 3. After feature selection using the LASSO regression shown in Supplementary Fig. 1, nine features with non-zero coefficients were included in the RAD score development. The type, filter, and coefficients of the final selected texture features are presented in Table 2, and a violin plot of the RAD score is shown in Supplementary Fig. 2. In both the training ($P < 0.001$) and test ($P = 0.002$) sets, the RAD score was higher in patients with LVAR than in those without LVAR.

Performance of Radiomics Score for Predicting LVAR

In the univariable logistic regression analysis, LVEF, infarct size, presence of MVO, and RAD score showed a significant predictive association with LVAR. After multivariable analysis, only infarct size (odds ratio [OR], 1.04; 95% confidence interval [CI], 1.00–1.07; $P = 0.031$) and the RAD score (OR, 3.43; 95% CI, 2.34–5.28; $P < 0.001$) were retained as independent predictors of LVAR (Table 3). The *best* cut-off values for predicting LVAR were RAD-score of 0.32, infarct size of 25.76% of the LV mass, and LVEF of 45%. A RAD score > 0.32 was related to an eight-fold increase in the LVAR probability (OR, 7.86; 95% CI, 3.55–18.66; $P < 0.001$).

https://doi.org/10.3348/kjr.2023.0061

Korean Journal of Radiology
KJR

Table 1. Characteristics of patients with STEMI in the training and testing set

Variables	Training set (n = 170)	Testing set (n = 74)	*P**
Demographic			
Age, yr	57.13 ± 10.57	56.61 ± 9.73	0.721
Sex, female	17 (10.0)	11 (14.9)	0.380
BMI, kg/m^2	25.91 ± 4.29	25.77 ± 3.75	0.811
Clinical status at recruitment			
Heart rate, bpm	78.35 ± 12.51	80.52 ± 13.88	0.229
Systolic BP, mmHg	125.09 ± 21.67	127.49 ± 21.67	0.427
Baseline Killip class			0.363
I	145 (85.3)	67 (90.5)	
> II	25 (14.7)	7 (9.5)	
Cardiovascular risk factors			
Hypertension	85 (50.0)	40 (54.1)	0.658
Diabetes mellitus	41 (24.1)	14 (18.9)	0.467
Hyperlipidemia	37 (21.8)	11 (14.9)	0.284
Procedural characteristics			
Time to reperfusion, h	13.08 ± 36.10	7.76 ± 13.13	0.219
MI location, non-anterior	91 (53.5)	34 (45.9)	0.342
Pre-procedural TIMI flow, 0–1	126 (74.1)	55 (74.3)	0.637
Post-procedural TIMI flow, 3	150 (88.2)	69 (93.2)	0.180
Laboratory examination			
CK-MB, ng/mL	87.8 (13.9–225.0)	59.1 (13.5–228.8)	0.518
hs-TnT, ng/mL	7.8 (1.8–100.0)	6.0 (1.0–99.8)	0.392
NT-ProBNP, pg/mL	146.0 (51.2–370.7)	196.4 (54.8–508.3)	0.455
Medication			
Aspirin	167 (98.2)	73 (98.6)	> 0.999
ACEI or ARB	138 (81.2)	63 (85.1)	0.573
β-blockers	141 (82.9)	62 (83.8)	> 0.999
Statin	167 (98.2)	73 (98.6)	> 0.999
CMR parameters			
LVEF, %	47.51 ± 10.49	48.23 ± 9.12	0.609
LV-EDV, mL	148.83 ± 38.94	148.47 ± 38.19	0.946
LGE-CMR parameters			
Infarct size, % of LV mass	23.92 ± 12.11	21.25 ± 10.94	0.104
Area at risk, % of LV mass	41.00 ± 15.81	37.30 ± 12.82	0.077
MVO	75 (44.1)	26 (35.1)	0.243
RAD score	0.00 ± 1.10	0.00 ± 1.04	> 0.999

Data are presented as count (%) for categorical variables and median (Q1–Q3) or mean ± standard deviation for continuous variables.
*Unpaired Student's *t*-test or Mann-Whitney U-test for continuous variables and chi-square test and Mann-Whitney U-test for categorical variables were applied to compare differences between groups.
STEMI = ST-segment elevation myocardial infarction, BMI = body mass index, BP = blood pressure, MI = myocardial infarction, TIMI = thrombolysis in myocardial infarction, CK-MB = creatine kinase MB, hs-TnT = high-sensitivity troponin T, NT-proBNP = N-terminal pro-B-type natriuretic peptide, ACEI = angiotensin converting enzyme inhibitor, ARB = angiotensin receptor blocker, CMR = cardiovascular magnetic resonance, LVEF = left ventricular ejection fraction, LV = left ventricular, EDV = end-diastolic volume, LGE = late gadolinium enhancement, MVO = microvascular obstruction, RAD = radiomics score

The AUC (95% CI) values for the RAD score, infarct size, and baseline LVEF to predict LVAR were, respectively, as follows: 0.82 (0.75–0.89), 0.61 (0.51–0.71), 0.65 (0.55–0.76) in the training set, and 0.75 (0.62–0.89), 0.75 (0.61–0.88), and 0.68 (0.52–0.84) in the testing set. The combination of infarct size and RAD score showed a favorable performance in predicting LVAR with an AUC of 0.83 (95% CI 0.76–0.90) under the training set and 0.84 (95% CI 0.72–0.95) for the testing set. As indicated in Table 4, the AUC of the combined RAD score and LVEF variable was

 https://doi.org/10.3348/kjr.2023.0061

0.83 (Model 1; 95% CI, 0.76–0.90), which was higher than for the combined MVO, infarct size, and LVEF (Model 2; 0.68; 95% CI, 0.59–0.78; Delong's test, $P = 0.007$) in the training set. In the testing set, the addition of the RAD score to LVEF increased the area under the curve (AUC; 95% CI) from 0.68 (0.52–0.84) to 0.82 (0.70–0.93) ($P = 0.018$). The AUC (95%

Table 2. Selected radiomics feature and coefficients

Features	Filter	Type	Coefficients
RAD score			
Least axis length	Original	Shape	-0.62192
Long run low gray level emphasis	Original	GLRLM	0.143564
Imc1	Gradient	GLCM	-0.16443
90 percentile	Lbp.3D.m2	Firstorder	0.029946
Dependence non-uniformity normalized	Square	GLDM	0.649632
Skewness	Wavelet.LLH	Firstorder	-0.2804
Run variance	Wavelet.LLH	GLRLM	0.142035
Idmn	Wavelet.HHH	GLCM	0.203119
Dependence non-uniformity normalized	Wavelet.HHH	GLDM	0.1062

RAD = radiomics score, Imc1 = information matrix correlation 1, Idmn = inverse deviation matrix normalization, GLRLM = grey-level run length matrix, GLCM = grey-level co-occurrence matrix, GLDM = grey-level dependence matrix

Table 3. Univariable and multivariable logistic regression analysis for LVAR

Variables	Univariable	*P*	Multivariable	*P*
	OR (95% CI)		OR (95% CI)	
Age, yr	1.01 (0.98–1.04)	0.475		
Sex, female	1.20 (0.45–2.87)	0.698		
Pre-procedural TIMI flow				
0–1	ref	-		
2	2.21 (0.70–6.48)	0.154		
3	0.47 (0.17–1.12)	0.111		
MI location, non-anterior	0.58 (0.31–1.07)	0.082		
Hypertension	1.67 (0.91–3.14)	0.102		
HDL, mmol/L	3.18 (1.04–9.74)	0.041		
NT-proBNP, pg/mL	1.02 (0.97–1.07)	0.34		
LVEF, %	0.95 (0.92–0.98)	< 0.001	0.96 (0.93–1.00)	0.057
Infarct size, % of LV mass	1.05 (1.02–1.08)	< 0.001	1.04 (1.00–1.07)	0.031
MVO	2.82 (1.53–5.32)	< 0.001		
RAD score	3.36 (2.32–5.07)	< 0.001	3.43 (2.34–5.28)	< 0.001

Only variables with a *P*-value < 0.05 in this univariable logistic regression were included in the multivariable logistic regression analysis with the stepwise forward method.
LVAR = left ventricular adverse remodeling, OR = odds ratio, CI = confidence interval, TIMI = thrombolysis in myocardial infarction, ref = reference, MI = myocardial infarction, HDL = high-density lipoproteins, NT-proBNP = N-terminal pro-B-type natriuretic peptide, LVEF = left ventricular ejection fraction, LV = left ventricular, MVO = microvascular obstruction, RAD = radiomics score

Table 4. Performance of combined models in predicting LVAR

Models	Training	*P*	Testing	*P*
	AUC (95% CI)		AUC (95% CI)	
LVEF	0.65 (0.55–0.76)		0.68 (0.52–0.84)	
RAD score	0.82 (0.75–0.89)		0.75 (0.62–0.89)	
Model 1: RAD score + LVEF	0.83 (0.76–0.90)	< 0.001*	0.82 (0.70–0.93)	0.018*
Model 2: LGE-CMR + LVEF	0.68 (0.59–0.78)	0.007†	0.79 (0.65–0.94)	0.727†

Features incorporated into the LGE-CMR + LVEF group included microvascular obstruction, infarct size, and LVEF.
*Comparison: Model 1 vs. LVEF, †Comparison: Model 1 vs. Model 2.
LVAR = left ventricular adverse remodeling, AUC = area under the curve, CI = confidence interval, LVEF = left ventricular ejection fraction, RAD = radiomics score, LGE = late gadolinium enhancement, CMR = cardiovascular magnetic resonance

https://doi.org/10.3348/kjr.2023.0061

Korean Journal of Radiology
KJR

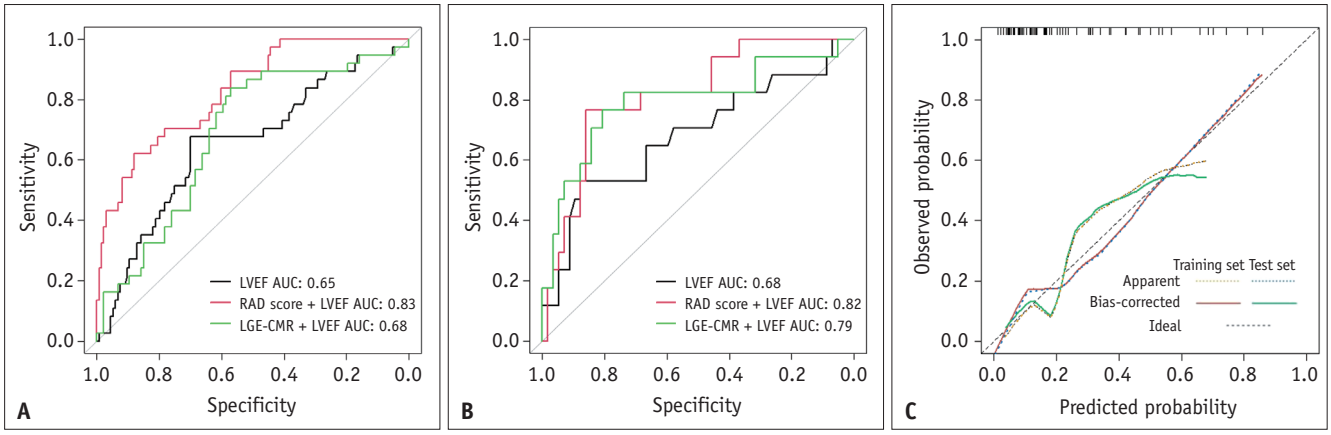

Fig. 2. Performance for predicting left ventricular adverse remodeling. Features incorporated into the LGE-CMR +LVEF group included microvascular obstruction, infarct size, and LVEF. ROC analyses for Adverse Remodeling versus No Adverse Remodeling in the training **(A)** and testing **(B)** datasets. The calibration curves demonstrate good calibration for predicting adverse LV remodeling in the training and testing sets **(C)**. LGE = late gadolinium enhancement, CMR = cardiovascular magnetic resonance, LVEF = left ventricular ejection fraction, ROC = receiver operating characteristic, LV = left ventricular, AUC = area under the curve, RAD = radiomics score

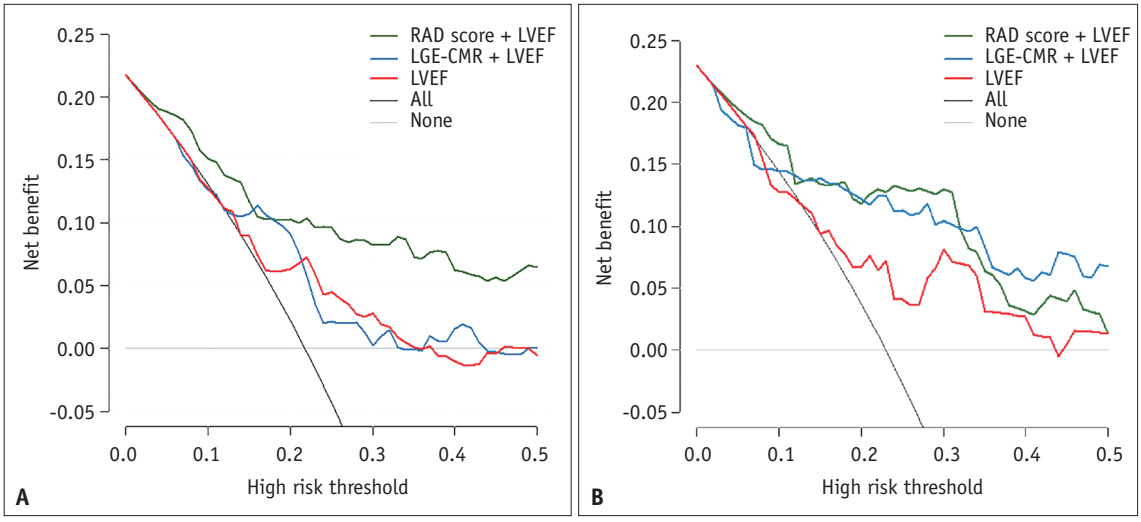

Fig. 3. Decision curve analysis for the RAD score + LVEF, LGE-CMR + LVEF and LVEF in predicting LVAR. Features incorporated into the LGE-CMR + LVEF group included microvascular obstruction, infarct size, and LVEF. Decision curve analysis for the models in predicting LVAR in the training **(A)** and testing **(B)** sets. RAD = radiomics score, LVEF = left ventricular ejection fraction, LGE = late gadolinium enhancement, CMR = cardiovascular magnetic resonance, LVAR = left ventricular adverse remodeling

CI) for the combined RAD score and LVEF was comparable to the addition of traditional CMR parameters (Model 2; AUC, 0.79; 95% CI, 0.65–0.94) (P = 0.727) to predict LVAR. The ROC curves for LGE-CMR + LVEF (MVO, infarct size, and LVEF), LVEF + RAD score, and RAD score are shown in Figure 2A, B. Good calibration to predict the LVAR obtained with the LVEF + RAD score variable in both the training and testing sets is shown in Figure 2C.

Besides, we have constructed models using logistic regression with five-fold cross-validation in the training set, during which "optuna" (https://optuna.org/) was used for searching optimal hyperparameters. The results for the training and testing sets were consistent with those of the random-split sample method (Supplementary Table 4). Decision curve analysis (DCA; Fig. 3) confirmed that the RAD score + LVEF yielded a greater net benefit from predicting LVAR than LVEF alone (both in the training and testing sets) and was comparable to the inclusion of LGE-CMR parameters (outperforming LGE-CMR + LVEF in the training set and comparable in the testing set) across the majority of the range of reasonable threshold probabilities.

The relationship between the nine selected radiomics

https://doi.org/10.3348/kjr.2023.0061

features, MVO, and infarct size was also evaluated. Only two of the nine radiomic features selected differed significantly between patients with and without MVO (Supplementary Fig. 3). By comparison, five features differed significantly between the high and low infarct size groups, classified according to the *best* cutoff infarct size value of > 25.76% LV mass (Supplementary Fig. 4).

DISCUSSION

In this study, we investigated the role of cine image-derived-radiomics in predicting LVAR following PCI in patients with acute STEMI. Radiomics features provided incremental values for LVEF alone in predicting LVAR. LVAR, characterized by eccentric hypertrophy and expansion of infarct size and LV volume, is associated with progressive heart failure after MI [2,3]. The association between adverse remodeling and all-cause mortality and heart failure varied by different cutoff values for LVAR. The definition of LVAR is essential when attempting to establish a predictive score or model. In this study, we followed the echocardiography-defined criteria (≥ 20% increase in LV-EDV from baseline), which have been widely used in CMR studies exploring the predictors of LVAR [19,22]. The extent of myocardial ischemia-reperfusion injury is a crucial determinant of LVAR and cardiovascular outcomes [6]. CMR provides comprehensive tissue characterization and functional analysis of the myocardium after MI. In patients with reperfused acute MI, CMR has been shown to track the remodeling process accurately [23]. Therefore, it is essential to consider the histological changes in the myocardium when assessing the risk of LVAR. However, LGE-CMR is contraindicated in patients with severe renal damage and involves difficulties that are challenging for both patients and radiologists, such as extended lying down and repeated breath-holding training during examinations. Using cine images to investigate potential prognostic information is of great value for simplifying CMR examinations and making them available to broader patients.

Advances in radiomics have recently paved the way for quantitative analysis of alterations in myocardial tissue, allowing medical images to be mined to extract quantitative features. Several studies have investigated the diagnostic performance of radiomic signatures in myocardial injuries. Chen et al. [24] demonstrated that radiomic signatures of extracellular volume fraction (ECV) mapping could distinguish between reversible and irreversible myocardial injuries, with an AUC of 0.91. Moreover, radiomic features of myocardial injury have been significantly associated with LVAR at the 6-month follow-up post-MI, with the combination of the radiomic signature of T1 mapping and T1 values providing a higher diagnostic value for MVO than T1 alone [25]. In patients with non-ischemic dilated cardiomyopathy, a study reported that a combination of T1 mapping-based radiomics features and LGE parameters accurately predicted the LVAR risk, with an AUC of 0.81 [26]. Notably, the radiomic features in that study were derived from a single T1 mapping image of the midventricular short axis. In contrast, our study defined a ROI encompassing multiple LV myocardial segments, and a portion of the extracted radiomic features was based on 3D analysis. In addition to the radiomic analysis of ECV and T1 mapping, radiomic signatures from cine images can be used to identify myocardial alterations post-MI at the tissue level. In comparison to scar size and location, Kotu et al. [27] showed that radiomic features extracted from LGE-CMR offer incremental value in predicting the risk of arrhythmias. However, few studies have investigated the value of radiomic analysis, particularly radiomic signatures extracted from non-contrast cine images, in predicting LVAR. To the best of our knowledge, this study is the first to explore an alternative method of radiomic analysis of non-contrast cine images to predict the risk of LVAR after PCI in patients with acute STEMI.

The quantitative characterization of pixel distribution in images, defined as radiomic signatures, offers new information on the relationship between individual heterogeneity and clinical outcomes. Our preliminary findings help define a unique radiomics signature to predict LVAR post-PCI after acute STEMI. The radiomics features included in our model were of three types: shape-based radiomics signatures, histogram-based first-order texture features, and spatial distributions of signal intensities. First-order texture features provide general signal intensity characteristics, whereas features such as the grey-level run length matrix (GLRLM) describe the spatial relationship between voxels [12]. However, we could not identify the precise relationship between radiomics features and histological changes because we did not directly associate these radiomics features with the histopathological alterations of the myocardium in our study.

Our findings indicate that cine image-based radiomic analysis of the myocardium is reliable and consistent. Our study followed a standard radiomics procedure by delineating multiple LV myocardial segments. Most previous radiomic analyses of CMR have been based on single or three cross-

https://doi.org/10.3348/kjr.2023.0061

Korean Journal of Radiology
KJR

sections, whereas information on the adjacent myocardium has been ignored [24,25,28,29]. Additionally, we performed LV myocardium segmentation semi-automatically using post-processing software and then masked the ROIs within the contour, which lowered the impact of artifacts related to the manual delineation of the ROIs. The RAD score yielded favorable performance in predicting LVAR after MI and thus may be a promising tool for identifying patients at higher risk for LVAR post-PCI after acute STEMI. To our knowledge, our study included one of the largest cohorts with follow-up CMR to investigate the association between radiomic signatures and LVAR.

The limitations of this study should be acknowledged. First, although our study included a sufficiently large sample size to develop a radiomics-based tool for assessing the risk of LVAR post-PCI after acute STEMI, selection bias cannot be ruled out, as all patients were treated at Chinese People's Liberation Army General Hospital and were retrospectively selected. Second, our radiomic analysis was performed at a single institution using a single type of MRI scanner (1.5T), which limits the generalizability of the study results. Therefore, prospective studies are required for the external validation of our findings and the generalizability of our radiomics model for clinical utility. The extracted radiomic features were based on end-diastolic LV myocardium and therefore did not account for previous findings of variability in radiomic features extracted at different times [30]. Therefore, the prognostic value of features extracted during other periods requires further study. Third, more clinical features such as soluble suppression of tumorigenesis-2 and other enzymatic markers during hospitalization have been reported as independent predictors of LVAR in Acute MI [31]. Although we could not consider all the previously reported features associated with LVAR, we included as many available predictors as possible. Future studies should compare radiomic analysis with other non-contrast techniques, such as T1 or T2 mapping techniques.

In summary, radiomics signatures from non-contrast cine CMR can predict LVAR after STEMI independently and incrementally to LVEF and may provide an alternative to traditional CMR parameters.

Supplement

The Supplement is available with this article at https://doi.org/10.3348/kjr.2023.0061.

Availability of Data and Material

The datasets generated or analyzed during the study are available from the corresponding author on reasonable request.

Conflicts of Interest

The authors have no potential conflicts of interest to disclose.

Author Contributions

Conceptualization: Xin A, Ying Zhang, Yundai Chen. Data curation: Xin A, Tong Chen. Formal analysis: Xin A, Mingliang Liu. Funding acquisition: Ying Zhang. Investigation: Xin A, Tong Chen, Geng Qian. Methodology: Xin A, Feng Chen. Project administration: Xin A, Geng Qian. Resources: Yundai Chen, Ying Zhang. Software: Xin A, Ying Zhang. Supervision: Yundai Chen. Validation: Yundai Chen. Visualization: Xin A. Writing—original draft: Xin A. Writing—review & editing: Yundai Chen.

ORCID IDs

Xin A
https://orcid.org/0000-0001-8637-1125
Mingliang Liu
https://orcid.org/0000-0002-5054-8870
Tong Chen
https://orcid.org/0000-0003-1951-0257
Feng Chen
https://orcid.org/0000-0003-1800-8441
Geng Qian
https://orcid.org/0000-0003-4201-3697
Ying Zhang
https://orcid.org/0000-0002-6199-6548
Yundai Chen
https://orcid.org/0000-0003-4409-9375

Funding Statement

This work was supported by National Natural and Science Foundation of China (No. 82000243).

REFERENCES

1. Symons R, Masci PG, Goetschalckx K, Doulaptsis K, Janssens S, Bogaert J. Effect of infarct severity on regional and global left ventricular remodeling in patients with successfully reperfused ST segment elevation myocardial infarction. *Radiology* 2015;274:93-102

2. Bolognese L, Neskovic AN, Parodi G, Cerisano G, Buonamici P, Santoro GM, et al. Left ventricular remodeling after primary coronary angioplasty: patterns of left ventricular dilation and long-term prognostic implications. *Circulation* 2002;106:2351-2357
3. Zile MR, Gaasch WH, Patel K, Aban IB, Ahmed A. Adverse left ventricular remodeling in community-dwelling older adults predicts incident heart failure and mortality. *JACC Heart Fail* 2014;2:512-522
4. Rodriguez-Palomares JF, Gavara J, Ferreira-González I, Valente F, Rios C, Rodríguez-García J, et al. Prognostic value of initial left ventricular remodeling in patients with reperfused STEMI. *JACC Cardiovasc Imaging* 2019;12:2445-2456
5. Nguyen TL, Phan J, Hogan J, Hee L, Moses D, Otton J, et al. Adverse diastolic remodeling after reperfused ST-elevation myocardial infarction: An important prognostic indicator. *Am Heart J* 2016;180:117-127
6. Westman PC, Lipinski MJ, Luger D, Waksman R, Bonow RO, Wu E, et al. Inflammation as a driver of adverse left ventricular remodeling after acute myocardial infarction. *J Am Coll Cardiol* 2016;67:2050-2060
7. Bulluck H, Rosmini S, Abdel-Gadir A, White SK, Bhuva AN, Treibel TA, et al. Residual myocardial iron following intramyocardial hemorrhage during the convalescent phase of reperfused ST-segment-elevation myocardial infarction and adverse left ventricular remodeling. *Circ Cardiovasc Imaging* 2016;9:e004940
8. Ibanez B, Aletras AH, Arai AE, Arheden H, Bax J, Berry C, et al. Cardiac MRI endpoints in myocardial infarction experimental and clinical trials: JACC scientific expert panel. *J Am Coll Cardiol* 2019;74:238-256
9. Liu D, Borlotti A, Viliani D, Jerosch-Herold M, Alkhalil M, De Maria GL, et al. CMR native T1 mapping allows differentiation of reversible versus irreversible myocardial damage in ST-segment-elevation myocardial infarction: an OxAMI Study (Oxford acute myocardial infarction). *Circ Cardiovasc Imaging* 2017;10:e005986
10. Savadjiev P, Chong J, Dohan A, Agnus V, Forghani R, Reinhold C, et al. Image-based biomarkers for solid tumor quantification. *Eur Radiol* 2019;29:5431-5440
11. Gillies RJ, Kinahan PE, Hricak H. Radiomics: images are more than pictures, they are data. *Radiology* 2016;278:563-577
12. Raisi-Estabragh Z, Izquierdo C, Campello VM, Martin-Isla C, Jaggi A, Harvey NC, et al. Cardiac magnetic resonance radiomics: basic principles and clinical perspectives. *Eur Heart J Cardiovasc Imaging* 2020;21:349-356
13. Avard E, Shiri I, Hajianfar G, Abdollahi H, Kalantari KR, Houshmand G, et al. Non-contrast Cine Cardiac Magnetic Resonance image radiomics features and machine learning algorithms for myocardial infarction detection. *Comput Biol Med* 2022;141:105145
14. Larroza A, López-Lereu MP, Monmeneu JV, Gavara J, Chorro FJ, Bodí V, et al. Texture analysis of cardiac cine magnetic resonance imaging to detect nonviable segments in patients with chronic myocardial infarction. *Med Phys* 2018;45:1471-1480
15. Larroza A, Materka A, López-Lereu MP, Monmeneu JV, Bodí V, Moratal D. Differentiation between acute and chronic myocardial infarction by means of texture analysis of late gadolinium enhancement and cine cardiac magnetic resonance imaging. *Eur J Radiol* 2017;92:78-83
16. Baessler B, Mannil M, Oebel S, Maintz D, Alkadhi H, Manka R. Subacute and chronic left ventricular myocardial scar: accuracy of texture analysis on nonenhanced cine MR images. *Radiology* 2018;286:103-112
17. Ibanez B, James S, Agewall S, Antunes MJ, Bucciarelli-Ducci C, Bueno H, et al. 2017 ESC guidelines for the management of acute myocardial infarction in patients presenting with ST-segment elevation: the Task Force for the management of acute myocardial infarction in patients presenting with ST-segment elevation of the European Society of Cardiology (ESC). *Eur Heart J* 2018;39:119-177
18. Lee JW, Hur JH, Yang DH, Lee BY, Im DJ, Hong SJ, et al. Guidelines for cardiovascular magnetic resonance imaging from the Korean Society of Cardiovascular Imaging-part 2: interpretation of cine, flow, and angiography data. *Korean J Radiol* 2019;20:1477-1490
19. Reindl M, Tiller C, Holzknecht M, Lechner I, Eisner D, Riepl L, et al. Global longitudinal strain by feature tracking for optimized prediction of adverse remodeling after ST-elevation myocardial infarction. *Clin Res Cardiol* 2021;110:61-71
20. van Griethuysen JJM, Fedorov A, Parmar C, Hosny A, Aucoin N, Narayan V, et al. Computational radiomics system to decode the radiographic phenotype. *Cancer Res* 2017;77:e104-e107
21. Zhou Y, Gu HL, Zhang XL, Tian ZF, Xu XQ, Tang WW. Multiparametric magnetic resonance imaging-derived radiomics for the prediction of disease-free survival in early-stage squamous cervical cancer. *Eur Radiol* 2022;32:2540-2551
22. Reindl M, Reinstadler SJ, Feistritzer HJ, Mueller L, Koch C, Mayr A, et al. Fibroblast growth factor 23 as novel biomarker for early risk stratification after ST-elevation myocardial infarction. *Heart* 2017;103:856-862
23. Mewton N, Roubille F, Bresson D, Prieur C, Bouleti C, Bochaton T, et al. Effect of colchicine on myocardial injury in acute myocardial infarction. *Circulation* 2021;144:859-869
24. Chen BH, An DA, He J, Wu CW, Yue T, Wu R, et al. Myocardial extracellular volume fraction radiomics analysis for differentiation of reversible versus irreversible myocardial damage and prediction of left ventricular adverse remodeling after ST-elevation myocardial infarction. *Eur Radiol* 2021;31:504-514
25. Ma Q, Ma Y, Yu T, Sun Z, Hou Y. Radiomics of non-contrast-enhanced T1 mapping: diagnostic and predictive performance for myocardial injury in acute ST-segment-elevation myocardial infarction. *Korean J Radiol* 2021;22:535-546
26. Chang S, Han K, Kwon Y, Kim L, Hwang S, Kim H, et al. T1 Map-based radiomics for prediction of left ventricular

https://doi.org/10.3348/kjr.2023.0061

reverse remodeling in patients with non-ischemic dilated cardiomyopathy. *Korean J Radiol* 2023;24:395-405
27. Kotu LP, Engan K, Borhani R, Katsaggelos AK, Ørn S, Woie L, et al. Cardiac magnetic resonance image-based classification of the risk of arrhythmias in post-myocardial infarction patients. *Artif Intell Med* 2015;64:205-215
28. Ma Q, Ma Y, Wang X, Li S, Yu T, Duan W, et al. A radiomics nomogram for prediction of major adverse cardiac events in ST-segment elevation myocardial infarction. *Eur Radiol* 2021;31:1140-1150
29. Baeβler B, Mannil M, Maintz D, Alkadhi H, Manka R. Texture analysis and machine learning of non-contrast T1-weighted MR images in patients with hypertrophic cardiomyopathy-preliminary results. *Eur J Radiol* 2018;102:61-67
30. Jang J, El-Rewaidy H, Ngo LH, Mancio J, Csecs I, Rodriguez J, et al. Sensitivity of myocardial radiomics features to imaging parameters in cardiac MR imaging. *J Magn Reson Imaging* 2021;54:787-794
31. Aimo A, Vergaro G, González A, Barison A, Lupón J, Delgado V, et al. Cardiac remodelling - Part 2: clinical, imaging and laboratory findings. A review from the study group on biomarkers of the heart failure association of the European Society of Cardiology. *Eur J Heart Fail* 2022;24:944-958

 https://doi.org/10.3348/kjr.2023.0061